

QCD radiative correction to color-octet J/ψ inclusive production at B Factories

Yu-Jie Zhang ^(a), Yan-Qing Ma ^(a), Kai Wang ^(a), and Kuang-Ta Chao ^(a,b)

(a) Department of Physics and State Key Laboratory of Nuclear Physics and Technology,

Peking University, Beijing 100871, China

(b) Center for High Energy Physics, Peking University, Beijing 100871, China

Abstract

In nonrelativistic Quantum Chromodynamics (NRQCD), we study the next-to-leading order (NLO) QCD radiative correction to the color-octet J/ψ inclusive production at B Factories. Compared with the leading-order (LO) result, the NLO QCD corrections are found to enhance the short-distance coefficients in the color-octet J/ψ production $e^+e^- \rightarrow c\bar{c}(^3P_0^{(8)} \text{ or } ^3P_0^{(8)})g$ by a factor of about 1.9. Moreover, the peak at the endpoint in the J/ψ energy distribution predicted at LO can be smeared by the NLO corrections, but the major color-octet contribution still comes from the large energy region of J/ψ . By fitting the latest data of $\sigma(e^+e^- \rightarrow J/\psi + X_{\text{non-}c\bar{c}})$ observed by Belle, we find that the values of color-octet matrix elements are much smaller than expected earlier by using the naive velocity scaling rules or extracted from fitting experimental data with LO calculations. As the most stringent constraint by setting the color-singlet contribution to be zero in $e^+e^- \rightarrow J/\psi + X_{\text{non-}c\bar{c}}$, we get an upper limit of the color-octet matrix element, $\langle 0 | \mathcal{O}^{J/\psi} [^1S_0^{(8)}] | 0 \rangle + 4.0 \langle 0 | \mathcal{O}^{J/\psi} [^3P_0^{(8)}] | 0 \rangle / m_c^2 < (2.0 \pm 0.6) \times 10^{-2} \text{ GeV}^3$ at NLO in α_s .

PACS numbers: 13.66.Bc, 12.38.Bx, 14.40.Pq

I. INTRODUCTION

It is widely believed that the heavy quarkonium production and annihilation decay can be described by an effective theory, non-relativistic quantum chromodynamics (NRQCD)[1]. In the NRQCD factorization approach, the production of a heavy quarkonium is described by a series of heavy quark pair states, which are produced at short-distances, and then evolve into the heavy quarkonium at long-distances by emitting or absorbing soft gluons. The long-distance NRQCD matrix elements are scaled by the relative velocity v between quark and antiquark in the quarkonium rest frame. And the heavy quark pair states at short-distances should not only have the same quantum numbers as those of the quarkonium, but also have other different quantum numbers. In particular, such heavy quark pairs can be in a color-octet state. This is the so called color-octet mechanism.

The color-octet scenario seems to acquire some significant successes in describing heavy quarkonium decay and production. But recently, several next-to-leading order (NLO) QCD corrections for the inclusive and exclusive heavy quarkonium production in the color-singlet piece are found to be large and significantly relieve the conflicts between the color-singlet model predictions and experiments. It may imply, though inconclusively, that the color-octet contributions in the production processes are not as big as previously expected, and the color-octet mechanism should be studied more carefully. Lots of work have been done to investigate the color-octet mechanism in NRQCD for heavy quarkonium production.

The current experimental results on J/ψ photoproduction cross sections at HERA seem to prefer the NLO color-octet predication [2], rather than the description of the NLO color-singlet piece [3, 4, 5, 6]. The DELPHI data favor the NRQCD color-octet mechanism for J/ψ production in $\gamma\gamma \rightarrow J/\psi X$ [7, 8].

The NLO QCD corrections to J/ψ and Υ production at the Tevatron and LHC were calculated including the color-singlet piece [9, 10, 11] and color octet piece [12]. The NLO color-singlet contributions are found to significantly enhance the cross sections especially in the large p_T region. The NLO QCD corrections to polarizations of J/ψ and Υ at the Tevatron and LHC were also calculated [12, 13, 14]. The QED contributions to the production of J/ψ there and NLO QCD corrections were also calculated [15, 16]. The NLO relativistic corrections to J/ψ production at the Tevatron and LHC were considered too [17]. The experimental data of polarizations favor the NLO QCD corrections of the color singlet piece

rather than the color octet piece. Recent developments and related topics in quarkonium production can be found in Refs. [18, 19, 20].

The charmonium production in e^+e^- annihilation at B factories has also provided an important test ground for NRQCD and color-octet mechanism. The large discrepancies of J/ψ production via double $c\bar{c}$ (including a hidden or an open charm pair) in e^+e^- annihilation at B factories between LO theoretical predictions[21, 22, 23],[24, 25] and experimental results [26, 27] once were challenging issues but now are largely resolved by higher order corrections: NLO QCD[28, 29, 30, 31, 32, 33, 34, 35] and relativistic [36, 37, 38, 39, 40] corrections, and the results show that the color-singlet NLO corrections (both in α_s and v) may increase the cross section of double charmonium production e.g. $e^+e^- \rightarrow J/\psi\eta_c$ by an order of magnitude, and indicate that the color-singlet contributions are overwhelmingly dominant in most cases and there seems no much room for the color-octet contributions in charmonium production in e^+e^- annihilation at B factories (discussions on the light-cone and other approaches can be seen in [41, 42, 43, 44]).

In the J/ψ inclusive production $e^+e^- \rightarrow J/\psi + X$ at B factories, there are two color-octet processes. One is $e^+e^- \rightarrow q\bar{q} + J/\psi + X (q = u, d, s)$ studied in Ref.[45], where the light quark q (or \bar{q}) emits a hard gluon which turns into a color-octet 3S_1 $c\bar{c}$ pair fragmenting into a J/ψ with soft hadrons. But the short-distance coefficient of this color-octet process was found to be negligible at $\sqrt{s} = 10.6$ GeV and can only be important at much higher energies than $\sqrt{s} = 10.6$ GeV[45]. Therefore, this process can be ignored at B factories.

The other color-octet process $e^+e^- \rightarrow c\bar{c}({}^3P_0^{(8)} \text{ or } {}^3P_0^{(8)})g$ was studied by Braaten and Chen[46]. Based on the LO NRQCD calculation, they predicted that the J/ψ production is dominated by the region near the upper endpoint in the J/ψ energy distribution, and the width of the peak near the endpoint is of the order of 150 MeV. But the measured J/ψ spectra in e^+e^- annihilation by BaBar [47] and Belle[48] do not exhibit any enhancement near the endpoint.

On the experimental side, the total prompt J/ψ cross sections in e^+e^- annihilation were measured to be $\sigma_{tot} = 2.52 \pm 0.21 \pm 0.21$ pb by BaBar [47], whereas Belle gave a much smaller value $\sigma_{tot} = 1.47 \pm 0.10 \pm 0.13$ pb [48]. Obviously, the large discrepancy between the two measurements should be further clarified. On the theoretical side, for the J/ψ inclusive production cross section, the color-singlet contributions including $e^+e^- \rightarrow J/\psi + gg$, $e^+e^- \rightarrow J/\psi + c\bar{c}$ and $e^+e^- \rightarrow J/\psi + q\bar{q}gg (q = u, d, s)$ at LO in α_s were estimated to be only

about $0.4 \sim 0.9$ pb [45, 49], which might imply that the color-octet contribution should play an important role in the inclusive J/ψ production[45]. However, the ratio of J/ψ production rate through double $c\bar{c}$ to that of J/ψ inclusive production measured by Belle[26]

$$R_{c\bar{c}} = \frac{\sigma[e^+e^- \rightarrow J/\psi + c\bar{c}]}{\sigma[e^+e^- \rightarrow J/\psi + X]} = 0.59_{-0.13}^{+0.15} \pm 0.12, \quad (1)$$

are much larger than LO NRQCD predictions. If only including the color-singlet contribution at LO in α_s , the ratio is about $0.2 \sim 0.4$ [45, 49]. And a large color-octet contribution to the J/ψ inclusive production would enhance the denominator and then further decrease this ratio. So, this became a very puzzling issue. Some theoretical studies have been suggested in resolving this problem. Fleming, Leibovich and Mehen use the Soft-Collinear Effective Theory (SCET) to resum the color-octet contribution[50]. Lin and Zhu use SCET to analyze the color-singlet contribution to $e^+e^- \rightarrow J/\psi gg$ [51]. Leibovich and Liu sum the leading and next-to-leading logarithms in the color-singlet contribution to the J/ψ production cross section[52]. As a new step, Zhang and Chao find the NLO QCD corrections to $e^+e^- \rightarrow J/\psi + c\bar{c}$ [31] to be large, and increase the cross sections by a factor of about 2 (using the same matrix elements as LO), making the ratio R larger than the LO results.

Very recently, Belle reported new measurements[53]

$$\sigma(e^+e^- \rightarrow J/\psi + X) = (1.17 \pm 0.02 \pm 0.07)pb, \quad (2)$$

$$\sigma(e^+e^- \rightarrow J/\psi + c\bar{c}) = (0.74 \pm 0.08_{-0.08}^{+0.09})pb, \quad (3)$$

$$\sigma(e^+e^- \rightarrow J/\psi + X_{non\ c\bar{c}}) = (0.43 \pm 0.09 \pm 0.09)pb. \quad (4)$$

The J/ψ inclusive production cross section given in Eq.(2) is significantly smaller than that given previously by BaBar[47] and Belle[48]. The double charm production cross section given in Eq.(3) also becomes smaller accordingly. The cross section of $J/\psi + X_{non\ c\bar{c}}$ includes the color-singlet contribution of $e^+e^- \rightarrow J/\psi + gg$ and the color-octet one of $e^+e^- \rightarrow c\bar{c}(^3P_0^{(8)} \text{ or } ^3P_0^{(8)})g$. The color-singlet piece has been investigated by including the NLO $O(\alpha_s)$ correction[34, 35] and $O(v^2)$ relativistic correction[40], of which each contributes an enhancement factor of $1.2 - 1.3$ to the cross section of $e^+e^- \rightarrow J/\psi + gg$. As a result, the color-singlet contribution has saturated the observed value given in Eq.(4), leaving little room for the color-octet contribution.

In order to further clarify this problem, it is certainly useful to study the color-octet process $e^+e^- \rightarrow c\bar{c}(^3P_0^{(8)} \text{ or } ^3P_0^{(8)})g$ itself and to examine the color-octet effect of the next-to-leading order (NLO) QCD correction on the J/ψ production at B factories. In this paper we will focus on the NLO QCD correction to the cross section and J/ψ energy distribution in $e^+e^- \rightarrow c\bar{c}(^3P_0^{(8)} \text{ or } ^3P_0^{(8)})g$. The paper is organized as follows. In Section II, we will calculate the leading order color-octet production cross sections. In Section III, we will calculate the NLO virtual and real corrections. In section IV, we will give the numerical results and relations to the color-octet matrix elements. A summary will be given in Section V.

II. LEADING ORDER CALCULATION

In the NRQCD factorization framework, we can write down the cross section for the J/ψ inclusive production as

$$d\sigma(e^+e^- \rightarrow J/\psi + X) = \sum_n d\hat{\sigma}(e^+e^- \rightarrow c\bar{c}[n] + X) \langle 0 | \mathcal{O}^{J/\psi}[n] | 0 \rangle, \quad (5)$$

Here $d\hat{\sigma}$ is the inclusive cross section for $c\bar{c}$ pair in a color and angular momentum state labeled by $[n] = ^{2S+1}L_J^{(i)}$ produced in e^+e^- annihilation. And S, L, J is the spin, orbit, and total angular momentum quantum numbers of the $c\bar{c}$, and $i = 1(8)$ means that $c\bar{c}$ is in color-singlet (octet) state. The short-distance coefficients are calculable in a perturbation series in α_s . The long-distance matrix elements $\langle \mathcal{O}_n^{J/\psi} \rangle$ are the vacuum matrix elements of four-fermion operators in NRQCD [1]. The long-distance matrix elements are scaled by the relative velocity $v \ll 1$ of the c and \bar{c} quarks in the $c\bar{c}$ rest frame.

At lowest order in v the only term in Eq. (5) is the color-singlet contribution, $[n] = ^3S_1^{(1)}$, which is scaled as $\mathcal{O}(v^3)$. The coefficient for this contribution starts at $\mathcal{O}(\alpha_s^2)$ [45, 49], and its contribution is away from the upper endpoint $E_{max} = (s + m_{J/\psi}^2)/(2\sqrt{s})$, where s is the center-of-mass energy squared[45]. The color-octet contributions also start at $\mathcal{O}(\alpha_s^2)$, but are suppressed by $v^4 \approx 0.1$ relative to the color-singlet contribution, and they are negligible in most of the allowed phase-space at leading order in perturbation theory. However, as it is pointed out in Ref. [46], there is an $\mathcal{O}(\alpha_s)$ contribution to color-octet production near the upper endpoint, for which the Feynman diagrams are shown in Fig. 1. Here $[n]$ is $^1S_0^{(8)}$ or $^3P_J^{(8)}$, and contributions of other Fock-states are suppressed by v^2 . The three P-wave matrix

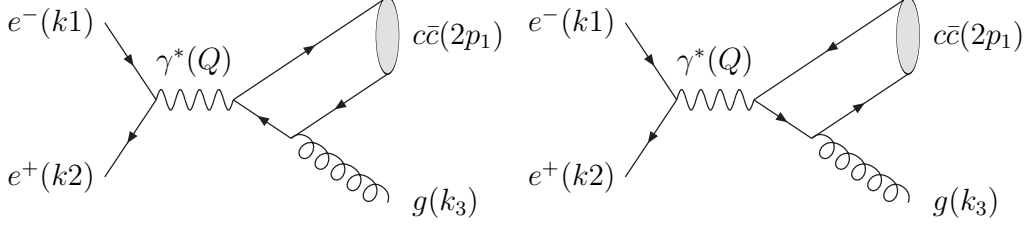


FIG. 1: Two Born diagrams for $e^- e^+ \rightarrow c\bar{c} + g$.

elements are not independent at leading order in v^2 , and are related by

$$\langle 0 | \mathcal{O}^{J/\psi} [{}^3P_J^{(8)}] | 0 \rangle = (2J + 1) \langle 0 | \mathcal{O}^{J/\psi} [{}^3P_0^{(8)}] | 0 \rangle (1 + \mathcal{O}(v^2)) \quad (6)$$

In the LO calculation, we refer to e.g. Ref [46]. Momenta for the involved particles are assigned as $e^-(k_1)e^+(k_2) \rightarrow c\bar{c}(2p_1) + g(k_3)$. In the calculation, we use `FeynArts` [54] to generate Feynman diagrams and amplitudes, `FeynCalc` [55] for the tensor reduction, and `LoopTools` [56] for the numerical evaluation of the infrared (IR)-safe one-loop integrals.

$d\hat{\sigma}$ is related to the amplitude of created charm quark pair in a color and angular momentum state $[n]$,

$$\begin{aligned} \mathcal{A}(e^+e^- \rightarrow c\bar{c}({}^{2S+1}L_J^{(8)})(2p_1) + g(k_3)) \\ = \sum_{L_z S_z} \sum_{s_1 s_2} \sum_{jk} \langle s_1; s_2 | SS_z \rangle \langle LL_z; SS_z | JJ_z \rangle \langle 3j; \bar{3}k | 8, a \rangle \times \\ \begin{cases} \mathcal{A}(e^+e^- \rightarrow c_j(p_1) + \bar{c}_k(p_1) + g(k_3)) & (L = S), \\ \left. \epsilon_\alpha^*(L_z) \frac{\partial}{\partial q^\alpha} \mathcal{A}(e^+e^- \rightarrow c_j(p_1 + q) + \bar{c}_k(p_1 - q) + g(k_3)) \right|_{q=0} & (L = P), \end{cases} \end{aligned} \quad (7)$$

where $\langle 3j; \bar{3}k | 8, a \rangle = \sqrt{2}T^a$, $\langle s_1; s_2 | SS_z \rangle$, $\langle LL_z; SS_z | JJ_z \rangle$ are respectively the color-SU(3), spin-SU(2), and angular momentum Clebsch-Gordan coefficients for the $c\bar{c}$ pairs projecting on appropriate bound states. $\mathcal{A}(e^+e^- \rightarrow c_j(p_1 + q) + \bar{c}_k(p_1 - q) + g(k_3))$ is the scattering amplitude for the $c\bar{c}$ production. We introduce the spin projection operators $P_{SS_z}(p, q)$ as[57]

$$P_{SS_z}(p, q) \equiv \sum_{s_1 s_2} \langle s_1; s_2 | SS_z \rangle v(p_1 - q; s_1) \bar{u}(p_1 + q; s_2). \quad (8)$$

Expanding $P_{SS_z}(p_1, q)$ in terms of the relative momentum q , we get the projection operators at leading term and next-to-leading term of q , which will be used in our calculation, as

follows

$$\begin{aligned}
P_{1S_z}(p_1, 0) &= \frac{1}{\sqrt{2}} \not{\epsilon}^*(S_z)(\not{p}_{1+} + m_c). \\
P_{00}(P, 0) &= \frac{1}{\sqrt{2}} \gamma_5(\not{p}_{1+} + m_c). \\
P_{1S_z}^\alpha(P, 0) &= \frac{1}{\sqrt{2}m_c} [\gamma^\alpha \not{\epsilon}^*(S_z)(\not{p}_{1+} + m_c) - (\not{p}_{1-} - m_c) \not{\epsilon}^*(S_z) \gamma^\alpha].
\end{aligned} \tag{9}$$

III. NEXT-TO-LEADING ORDER CORRECTIONS

To the next-to-leading order in α_s , the cross section is

$$\sigma = \sigma_{Born} + \sigma_{virtual} + \sigma_{real} + \mathcal{O}(\alpha^2 \alpha_s^3), \tag{10}$$

where

$$\begin{aligned}
d\sigma_{Born} &= \frac{1}{4} \frac{1}{2s} \sum |\mathcal{M}_{Born}|^2 dPS_2 \\
d\sigma_{virtual} &= \frac{1}{4} \frac{1}{2s} \sum 2 \operatorname{Re}(\mathcal{M}_{Born}^* \mathcal{M}_{NLO}) dPS_2 \\
d\sigma_{real} &= \frac{1}{4} \frac{1}{2s} \sum |\mathcal{M}_{real}|^2 dPS_3.
\end{aligned} \tag{11}$$

The factor $1/4$ is the average over spins of initial states. The factor $1/2s$ is the flux factor. \sum means summation over the polarizations of initial and final states. Then we need calculate \mathcal{M}_{NLO} . Here $dPS_{2(3)}$ means two(three) body phase space. Then the self-energy and triangle diagrams are all corresponding to propagators and vertexes of born diagrams. A half of the counter term, self energy, and vertex Feynman diagrams for $e^-(k_1)e^+(k_2) \rightarrow c\bar{c}(2p_1)g(k_3)$ are shown in FIG.2. Other diagrams can be obtained by reversing the quark lines. And the box Feynman diagrams are shown in FIG.3.

At NLO in α_s , there are ultraviolet(UV), infrared(IR), and Coulomb singularities. We choose $D = 4 - 2\epsilon$ dimension and relative velocity v to regularize UV, IR, and Coulomb singularities. The self energy and vertex Feynman diagrams contain UV singularities, which should be removed by renormalization. The renormalization constants of the QCD gauge

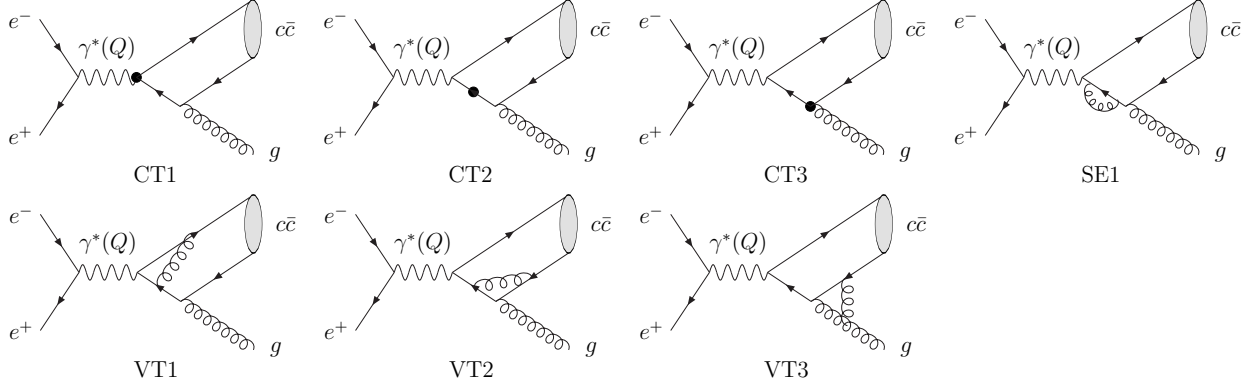


FIG. 2: Half of the counter term, self energy, and vertex Feynman diagrams for $e^-(k_1)e^+(k_2) \rightarrow c\bar{c}(2p_1)g(k_3)$.

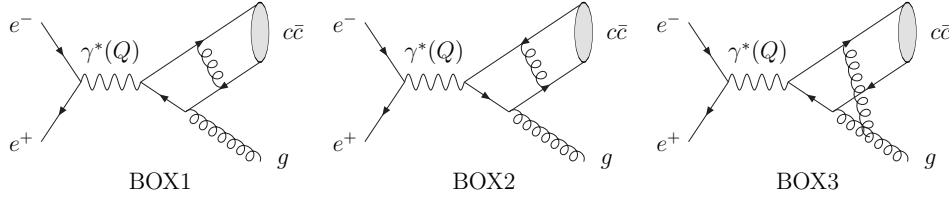


FIG. 3: Three box Feynman diagrams for $e^-(k_1)e^+(k_2) \rightarrow c\bar{c}(2p_1)g(k_3)$.

coupling constant $g_s = \sqrt{4\pi\alpha_s}$, the charm-quark mass m and field ψ , and the gluon field A_μ are defined as

$$g_s^0 = Z_g g_s, \quad m^0 = Z_m m, \quad \psi^0 = \sqrt{Z_2} \psi, \quad A_\mu^0 = \sqrt{Z_3} A_\mu. \quad (12)$$

Here the superscript 0 means bare quantities and the renormalization constants $Z_i = 1 + \delta Z_i$ with $i = g, m, 2, 3$. In the NLO calculation, the precision of the quantities δZ_i should be $\mathcal{O}(\alpha_s)$. We choose Z_2 , Z_3 , and Z_m in the on-mass-shell (OS) scheme, and Z_g in the the modified minimal-subtraction ($\overline{\text{MS}}$) scheme

$$\begin{aligned} \delta Z_2^{\text{OS}} &= -C_F \frac{\alpha_s}{4\pi} \left[\frac{1}{\epsilon_{\text{UV}}} + \frac{2}{\epsilon_{\text{IR}}} - 3\gamma_E + 3 \ln \frac{4\pi\mu^2}{m^2} + 4 \right] + \mathcal{O}(\alpha_s^2), \\ \delta Z_m^{\text{OS}} &= -3C_F \frac{\alpha_s}{4\pi} \left[\frac{1}{\epsilon_{\text{UV}}} - \gamma_E + \ln \frac{4\pi\mu^2}{m^2} + \frac{4}{3} \right] + \mathcal{O}(\alpha_s^2), \\ \delta Z_3^{\text{OS}} &= \frac{\alpha_s}{4\pi} (\beta_0 - 2C_A) \left[\frac{1}{\epsilon_{\text{UV}}} - \frac{1}{\epsilon_{\text{IR}}} \right] + \mathcal{O}(\alpha_s^2), \\ \delta Z_g^{\overline{\text{MS}}} &= -\frac{\beta_0}{2} \frac{\alpha_s}{4\pi} \left[\frac{1}{\epsilon_{\text{UV}}} - \gamma_E + \ln(4\pi) \right] + \mathcal{O}(\alpha_s^2), \end{aligned} \quad (13)$$

where μ is the renormalization scale, γ_E is the Euler's constant and $\beta_0 = (11/3)C_A - (4/3)T_F n_f$ is the one-loop coefficient of the QCD beta function, and n_f is the number of

active quark flavors. There are three massless light quarks u, d, s so $n_f = 3$. The charm quark c is not included in the running coupling[3]. In this scheme, we do not need to calculate the self-energy on external quark and gluon legs. Color factors are given by $T_F = 1/2, C_F = 4/3, C_A = 3$ in $SU(3)_c$.

Since we are calculating the NLO corrections to the LO cross section, which is already of $\mathcal{O}(\alpha_s)$, we have to employ the two-loop formula for $\alpha_s(\mu)$,

$$\frac{\alpha_s(\mu)}{4\pi} = \frac{1}{\beta_0 L} - \frac{\beta_1 \ln L}{\beta_0^3 L^2}, \quad (14)$$

where $L = \ln(\mu^2/\Lambda_{\text{QCD}}^2)$, and $\beta_1 = (34/3)C_A^2 - 4C_F T_F n_f - (20/3)C_A T_F n_f$ is the two-loop coefficient of the QCD beta function.

Exchange of the longitudinal gluon between external charm quark pair in Feynman diagram BOX1 and BOX2 of FIG.3 should lead to the Coulomb singularities $1/v$, where v is the relative velocity in the $c\bar{c}$ rest frame. For the Coulomb-singular color-octet process, we find

$$d\sigma = \langle \mathcal{O}_n^{J/\psi} \rangle_{LO} d\hat{\sigma}^{(0)} \left(1 - \frac{\pi\alpha_s}{6v} + \frac{\alpha_s \hat{C}}{\pi} + \mathcal{O}(\alpha_s^2) \right). \quad (15)$$

The NLO color-octet matrix element $\langle \mathcal{O}_n^{J/\psi} \rangle$ are proportional to $\pi\alpha_s/(6v)$ [1]. It is just the Coulomb-singular term in Eq. (15). So that

$$d\sigma = \langle \mathcal{O}_n^{J/\psi} \rangle_{NLO} d\hat{\sigma}^{(0)} \left(1 + \frac{\alpha_s \hat{C}}{\pi} + \mathcal{O}(\alpha_s^2) \right). \quad (16)$$

Then the contribution of Coulomb singularity has to be factored out and mapped into the color-octet matrix element $\langle \mathcal{O}_n^{J/\psi} \rangle$.

The Feynman Diagrams in FIG.3 and VT3 in FIG.2 contain IR singularity. LoopTools can not deal with IR divergent function and five point function, so we need calculate it by hand. We can separate the divergence through the way in Ref.[58]. Then all the IR singular parts become $C_0[-k_3, p_1, 0, 0, m]$ and $C_0[p_1, -p_1, 0, m, m]$, which are defined as

$$C_0[p_1, p_2, m_0, m_1, m_2] = \int \frac{\mu^{2\epsilon} d^D q}{(2\pi)^D} \frac{1}{[q^2 - m_0^2][(q+p_1)^2 - m_1^2][(q+p_2)^2 - m_2^2]}. \quad (17)$$

$C_0[p_1, -p_1, 0, m, m]$ contains soft and Coulomb singularities, and it will appear in Box1 and Box2 that are shown in FIG.3. It can be regularized by $D = 4 - 2\epsilon$ space-time dimension and relative velocity v :

$$C_0[p_1, -p_1, 0, m, m] = \frac{-i}{2m^2(4\pi)^2} \left(\frac{4\pi\mu^2}{m^2} \right)^\epsilon \Gamma(1+\epsilon) \left[\frac{1}{\epsilon} + \frac{\pi^2}{v} - 2 + \mathcal{O}(\epsilon) \right], \quad (18)$$

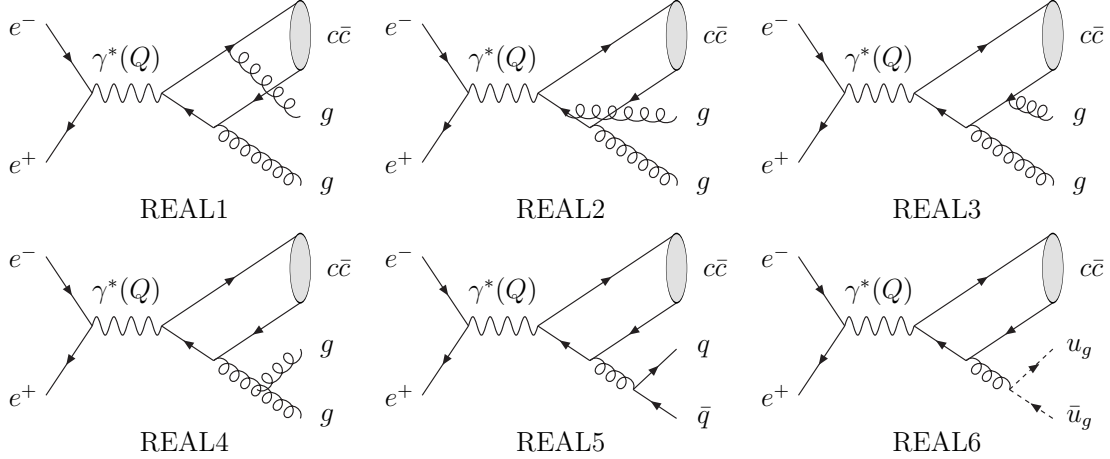


FIG. 4: Six of the twelve real correction diagrams.

where $v = \sqrt{-(p_{1c} - p_{1\bar{c}})^2}/m$. In the meson rest frame, we have $v = |\vec{p}_{1c} - \vec{p}_{1\bar{c}}|/m$, which is just the relative velocity v between c and \bar{c} . $C_0[-k_3, p_1, 0, 0, m]$ has soft and collinear singularities, and it will appear in VT3 in FIG.2 and Box3 in FIG.3.

$$C(-k_3, -k_3 - p, 0, 0, m) = \frac{i e^{-\epsilon(\gamma_E - \ln 4\pi)}}{16\pi^2} \left(\frac{\mu^2}{m^2}\right)^\epsilon \frac{1}{4p_1 \cdot k_3} \left[\frac{1}{\epsilon^2} - \frac{2}{\epsilon} \ln\left(\frac{-2p_1 \cdot k_3}{m^2}\right) + 2 \ln^2\left(\frac{-2p_1 \cdot k_3}{m^2}\right) + 2\text{Li}_2\left(\frac{2p_1 \cdot k_3 + m^2}{m^2}\right) + \frac{1}{2}\zeta(2) \right]. \quad (19)$$

There are twelve diagrams for real corrections, six diagrams for gg process, two for $q\bar{q}$ process, and two for ghost process. Half of them are shown in Fig.4. The other six diagrams can be gotten through reversing the charm quark lines. The calculation of the real corrections is similar to the leading order calculation, but there should appear IR singularities. [59].

IV. NUMERICAL RESULT AND COLOR-OCTET MATRIX ELEMENTS

We now turn to numerical calculations for the cross sections. Taking $m_{J/\psi} = 2m$, $m = 1.55$ GeV, $\Lambda_{\overline{\text{MS}}}^{(3)} = 388$ MeV, then $\alpha_s(\mu) = 0.245$ for $\mu = 2m$. The cross section at LO in α_s is

$$\sigma(e^+ + e^- \rightarrow J/\psi + X) = \left[11 \frac{\langle 0 | \mathcal{O}^{J/\psi} [^1S_0^{(8)}] | 0 \rangle}{\text{GeV}^3} + 18 \frac{\langle 0 | \mathcal{O}^{J/\psi} [^3P_0^{(8)}] | 0 \rangle}{\text{GeV}^5} \right] \text{pb}; \quad (20)$$

while the cross section at NLO in α_s becomes

$$\sigma(e^+ + e^- \rightarrow J/\psi + X) = \left[21 \frac{\langle 0 | \mathcal{O}^{J/\psi} [^1S_0^{(8)}] | 0 \rangle}{\text{GeV}^3} + 35 \frac{\langle 0 | \mathcal{O}^{J/\psi} [^3P_0^{(8)}] | 0 \rangle}{\text{GeV}^5} \right] \text{pb}. \quad (21)$$

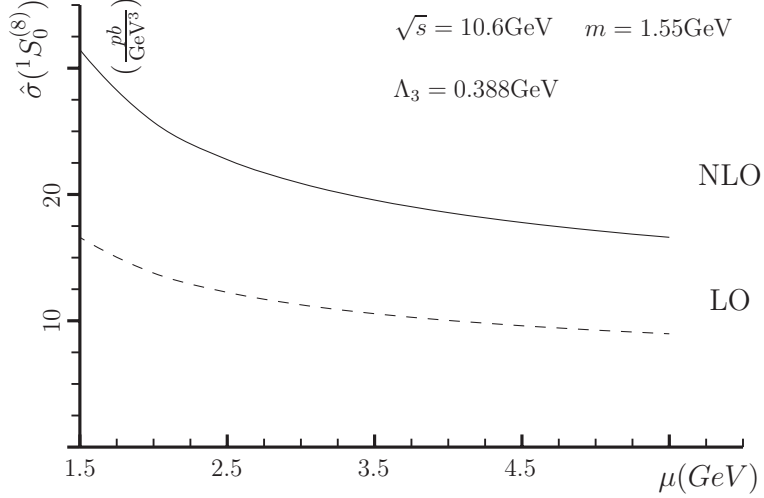


FIG. 5: The short-distance coefficient $\hat{\sigma}(^1S_0^{(8)})$ in $e^+e^- \rightarrow c\bar{c}(^1S_0^{(8)})g$ as functions of the renormalization scale μ .

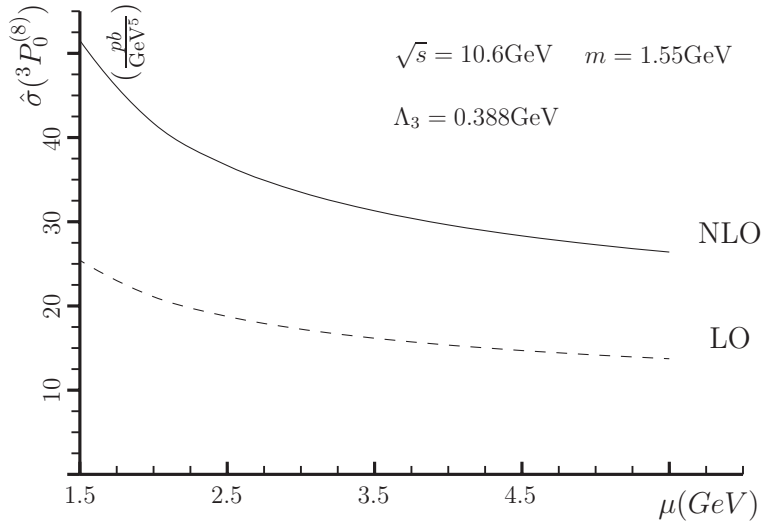


FIG. 6: The short-distance coefficient $\hat{\sigma}(^3P_0^{(8)})$ in $e^+e^- \rightarrow c\bar{c}(^3P_0^{(8)})g$ as functions of the renormalization scale μ .

The NLO short-distance coefficients are larger than the LO coefficients by a factor of about 1.9. Our LO result is consistent with that in Ref.[46]. Dependence of the short-distance coefficient $\hat{\sigma}(^1S_0^{(8)})$ on the renormalization scale μ is shown in FIG.5, and $\hat{\sigma}(^3P_0^{(8)})$ is shown in FIG.6.

If we choose an energy cut E_{cut} for the J/ψ in the endpoint region, we can get the cross section $\sigma|_{E_{J/\psi} > E_{CUT}}$. The result for $c\bar{c}(^1S_0^{(8)})$ is shown in FIG. 7 and the result for $c\bar{c}(^3P_J^{(8)})$

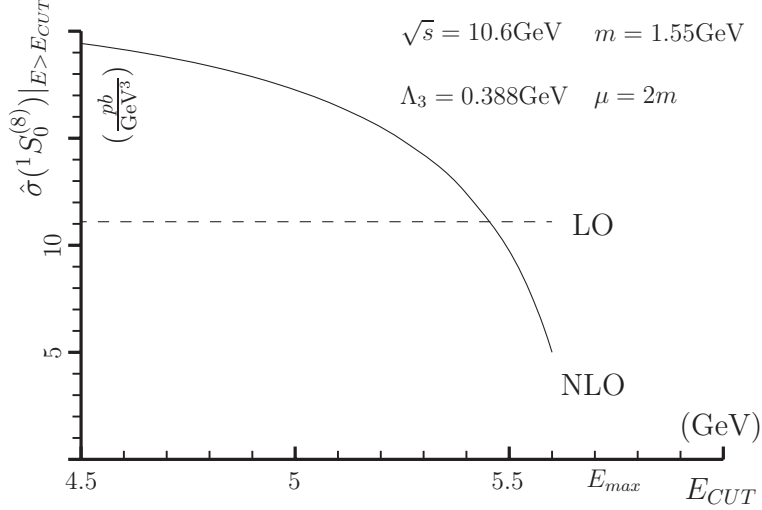


FIG. 7: The short-distance coefficient $\hat{\sigma}(^1S_0^{(8)})|_{E_{J/\psi}>E_{CUT}}$ in $e^+e^- \rightarrow c\bar{c}(^1S_0^{(8)})g$ as functions of the $c\bar{c}$ energy cut E_{CUT} .

shown in FIG. 8. We see that at LO the short-distance coefficients only contribute when the J/ψ energy is near the endpoint, and the NLO QCD correction can, to some extent, smear the J/ψ energy distribution near the endpoint. Nevertheless, at NLO the most color-octet contribution still comes from the large energy region, say $E > 5$ GeV. The evolution from the short-distance color-octet $c\bar{c}$ to the final state J/ψ should affect the distribution of J/ψ energy via emitting or absorbing soft gluons. If we ignore this effect, the distribution of J/ψ energy in e^+e^- center of momentum frame is a delta function $\delta(E - E_{max})$ and $E_{max} = (s + m_{J/\psi}^2)/(2\sqrt{s})$ at LO. Braaten and Chen analyzed this evolution effect, and it might broaden the energy distribution in the order of 150 MeV[46]. But it does not change the fact that most of the color-octet contributions concentrate on the large energy J/ψ region. Experimentally, the observed cross sections do not exhibit any enhancement near the endpoint[47, 48].

The color-octet matrix element

$$M_k = \langle 0 | \mathcal{O}^{J/\psi} [^1S_0^{(8)}] | 0 \rangle + k \langle 0 | \mathcal{O}^{J/\psi} [^3P_0^{(8)}] | 0 \rangle / m_c^2 \quad (22)$$

was previously extracted from the Tevatron data for J/ψ production with the LO calculations, which is listed in Table.I. If we use the minimum value of the matrix element, $M_{3.5} = 4.54 \times 10^{-2} \text{GeV}^3$, we can get the cross section at LO in α_s from Eq.(20)

$$\sigma(e^+ + e^- \rightarrow J/\psi + X) = (0.50 \sim 0.55) \text{pb}, \quad (23)$$

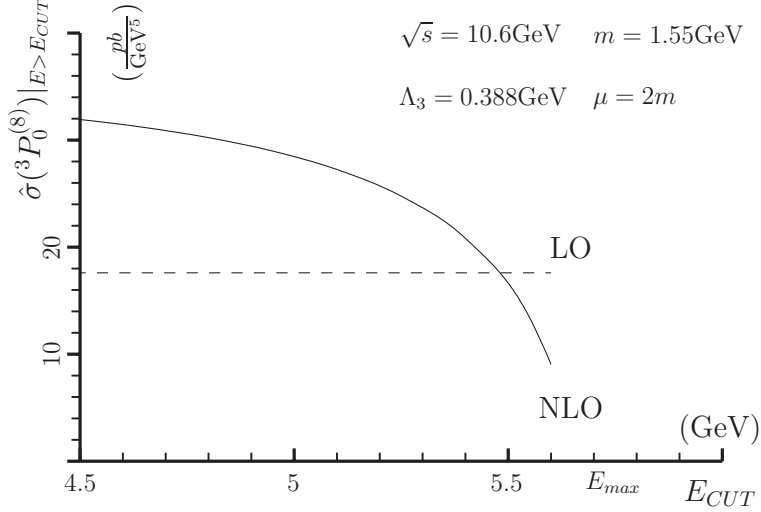


FIG. 8: The short-distance coefficient $\hat{\sigma}(^3P_0^{(8)})|_{E_{J/\psi}>E_{CUT}}$ in $e^+e^- \rightarrow c\bar{c}(^3P_0^{(8)})g$ as functions of the $c\bar{c}$ energy cut E_{CUT} .

TABLE I: Color-octet matrix elements $M_k = \langle 0|\mathcal{O}^{J/\psi}[^1S_0^{(8)}]|0\rangle + k\langle 0|\mathcal{O}^{J/\psi}[^3P_0^{(8)}]|0\rangle/m_c^2$

| | k | $M_k(10^{-2}\text{GeV}^3)$ |
|-------------------------------------|-----|----------------------------|
| Cho and Leibovich [60, 61] | 3 | 6.5 ± 1.5 |
| Braaten, <i>et al.</i> MRST98LO[62] | 3.4 | 8.7 ± 0.9 |
| Braaten, <i>et al.</i> CTEQ5L[62] | 3.4 | 6.6 ± 0.7 |
| Kramer [63] | 3.5 | 4.54 ± 1.11 |

and the cross section at NLO in α_s from Eq.(21)

$$\sigma(e^+ + e^- \rightarrow J/\psi + X) = (0.93 \sim 1.08)\text{pb}. \quad (24)$$

The calculated cross section in Eq.(24) for this color-octet process, which belongs to the $J/\psi + X_{non\ c\bar{c}}$ production, is much larger than the latest observed value given in Eq.(4): $\sigma[J/\psi + X_{non\ c\bar{c}}] = 0.43 \pm 0.13$ pb [53].

In fact, for the $e^+e^- \rightarrow J/\psi + X_{non\ c\bar{c}}$ production, the color-singlet process $e^+e^- \rightarrow J/\psi + gg$ has been found to make a dominant contribution to the cross section: $\sigma(e^+e^- \rightarrow J/\psi + gg) = 0.4 \sim 0.7$ pb at NLO in α_s and v^2 [34, 35, 40], thus leaves little room to the color-octet contributions. This gives a very stringent constraint on the color-octet contribution, and may imply that the values of color-octet matrix elements are much smaller than expected earlier by using the naive velocity scaling rules or extracted from fitting experimental data

with the leading-order calculations.

Even if we disregard the dominant contribution of $e^+e^- \rightarrow J/\psi + gg$ to $e^+e^- \rightarrow [J/\psi + X_{non\ c\bar{c}}]$ by setting the color-singlet contribution $\sigma(e^+e^- \rightarrow J/\psi + gg)$ to be zero, and combining Eq.(4) with Eq.(21), we can get an upper bound of the color-octet matrix element:

$$M_{4.0}^{NLO} < (2.0 \pm 0.6) \times 10^{-2} \text{ GeV}^3 \quad (25)$$

All the values of the color-octet matrix elements listed in Tab.I are larger than this upper bound by at least a factor of 2 .

V. SUMMARY

In summary, we find that the NLO QCD radiative corrections can enhance the short distance coefficient of color-octet J/ψ production at B factories via $e^+e^- \rightarrow c\bar{c}(^1S_0^{(8)} \text{ or } ^3P_0^{(8)})g$ with a K factor (the ratio of cross sections of NLO to LO) of about 1.9. The NLO QCD correction smears the J/ψ energy distribution near the endpoint. But the most color-octet contribution is still from the large energy region. The values of color-octet matrix elements are much smaller than expected earlier by using the naive velocity scaling rules or extracted from fitting the experimental data with the leading-order calculations. If we ignore the dominant color-singlet contribution by setting the color-singlet contribution to be zero, and use the color-octet contribution to saturate the latest observed production cross section $\sigma(e^+e^- \rightarrow J/\psi + X_{non\ c\bar{c}})$, we get the most stringent upper bound for the color-octet matrix element: $\langle 0 | \mathcal{O}^{J/\psi} [^1S_0^{(8)}] | 0 \rangle + 4.0 \langle 0 | \mathcal{O}^{J/\psi} [^3P_0^{(8)}] | 0 \rangle / m_c^2 < (2.0 \pm 0.6) \times 10^{-2} \text{ GeV}^3$ at NLO in α_s .

Acknowledgments

We thank G. Bodwin for useful comments. This work was supported by the National Natural Science Foundation of China (No 10805002, No 10675003, No 10721063) and the

- [1] G. T. Bodwin, E. Braaten, and G. P. Lepage, Phys. Rev. D **51**, 1125 (1995) [Erratum-ibid. D **55**, 5853 (1997)] [arXiv:hep-ph/9407339].
- [2] M. Butenschoen and B. A. Kniehl, arXiv:0909.2798 [hep-ph].
- [3] M. Kramer, Nucl. Phys. B **459**, 3 (1996) [arXiv:hep-ph/9508409].
- [4] C. H. Chang, R. Li and J. X. Wang, arXiv:0901.4749 [hep-ph].
- [5] P. Artoisenet, J. M. Campbell, F. Maltoni and F. Tramontano, arXiv:0901.4352 [hep-ph].
- [6] R. Li and K. T. Chao, Phys. Rev. D **79**, 114020 (2009) [arXiv:0904.1643 [hep-ph]].
- [7] M. Klasen, B. A. Kniehl, L. N. Mihaila and M. Steinhauser, Phys. Rev. Lett. **89**, 032001 (2002) [arXiv:hep-ph/0112259].
- [8] J. Abdallah *et al.* [DELPHI Collaboration], Phys. Lett. B **565**, 76 (2003) [arXiv:hep-ex/0307049].
- [9] P. Artoisenet, J. P. Lansberg and F. Maltoni, Phys. Lett. B **653**, 60 (2007) [arXiv:hep-ph/0703129].
- [10] J. Campbell, F. Maltoni and F. Tramontano, Phys. Rev. Lett. **98**, 252002 (2007) [arXiv:hep-ph/0703113].
- [11] R. Li and J. X. Wang, Phys. Lett. B **672**, 51 (2009) [arXiv:0811.0963 [hep-ph]].
- [12] B. Gong, X. Q. Li and J. X. Wang, arXiv:0805.4751 [hep-ph].
- [13] B. Gong and J. X. Wang, arXiv:0805.2469 [hep-ph].
- [14] B. Gong and J. X. Wang, arXiv:0802.3727 [hep-ph].
- [15] Z. G. He, R. Li and J. X. Wang, arXiv:0904.2069 [hep-ph].
- [16] Z. G. He, R. Li and J. X. Wang, arXiv:0904.1477 [hep-ph].
- [17] Y. Fan, Y. Q. Ma and K. T. Chao, arXiv:0904.4025 [hep-ph].
- [18] N. Brambilla *et al.*, arXiv:hep-ph/0412158.
- [19] J. P. Lansberg, Int. J. Mod. Phys. A **21**, 3857 (2006) [arXiv:hep-ph/0602091].
- [20] J. P. Lansberg *et al.*, arXiv:0807.3666 [hep-ph].
- [21] E. Braaten and J. Lee, Phys. Rev. D **67**, 054007 (2003) [Erratum-ibid. D **72**, 099901 (2005)] [arXiv:hep-ph/0211085].
- [22] K. Y. Liu, Z. G. He and K. T. Chao, Phys. Lett. B **557**, 45 (2003) [arXiv:hep-ph/0211181].

- K. Y. Liu, Z. G. He and K. T. Chao, Phys. Rev. D **77**, 014002 (2008).
- [23] K. Hagiwara, E. Kou and C. F. Qiao, Phys. Lett. B **570**, 39 (2003) [arXiv:hep-ph/0305102].
- [24] K. Y. Liu, Z. G. He and K. T. Chao, Phys. Rev. D **68**, 031501(R) (2003) [arXiv:hep-ph/0305084].
- [25] K. Y. Liu, Z. G. He and K. T. Chao, Phys. Rev. D **69**, 094027 (2004) [arXiv:hep-ph/0301218].
- [26] K. Abe *et al.* [BELLE Collaboration], Phys. Rev. Lett. **89**, 142001 (2002). [arXiv:hep-ex/0205104].
- [27] B. Aubert *et al.* [BABAR Collaboration], Phys. Rev. D **72**, 031101 (2005) [arXiv:hep-ex/0506062].
- [28] Y. J. Zhang, Y. J. Gao and K. T. Chao, Phys. Rev. Lett. **96**, 092001 (2006) [arXiv:hep-ph/0506076].
- [29] B. Gong and J. X. Wang, Phys. Rev. D **77**, 054028 (2008) [arXiv:0712.4220 [hep-ph]].
- [30] Y. J. Zhang, Y. Q. Ma and K. T. Chao, Phys. Rev. D **78**, 054006 (2008) [arXiv:0802.3655 [hep-ph]].
- [31] Y. J. Zhang and K. T. Chao, Phys. Rev. Lett. **98**, 092003 (2007) [arXiv:hep-ph/0611086].
- [32] B. Gong and J. X. Wang, arXiv:0904.1103 [hep-ph].
- [33] B. Gong and J. X. Wang, Phys. Rev. Lett. **100**, 181803 (2008) [arXiv:0801.0648 [hep-ph]].
- [34] Y. Q. Ma, Y. J. Zhang and K. T. Chao, Phys. Rev. Lett. **102**, 162002 (2009) [arXiv:0812.5106 [hep-ph]].
- [35] B. Gong and J. X. Wang, Phys. Rev. Lett. **102**, 162003 (2009) [arXiv:0901.0117 [hep-ph]].
- [36] Z. G. He, Y. Fan and K. T. Chao, Phys. Rev. D **75**, 074011 (2007) [arXiv:hep-ph/0702239].
- [37] G. T. Bodwin, J. Lee and C. Yu, Phys. Rev. D **77**, 094018 (2008) [arXiv:0710.0995 [hep-ph]].
- [38] G. T. Bodwin, D. Kang, T. Kim, J. Lee and C. Yu, AIP Conf. Proc. **892**, 315 (2007) [arXiv:hep-ph/0611002].
- [39] E. N. Elekina and A. P. Martynenko, arXiv:0910.0394 [hep-ph].
- [40] Z. G. He, Y. Fan and K. T. Chao, arXiv:0910.3636 [hep-ph].
- [41] J.P. Ma and Z.G. Si, Phys. Rev. D **70**, 074007(2004); Phys. Lett. B **647**,419 (2007).
- [42] V. V. Braguta, A. K. Likhoded and A. V. Luchinsky, Phys. Rev. D **78**, 074032 (2008) [arXiv:0808.2118 [hep-ph]]; V. V. Braguta, Phys. Rev. D **78**, 054025 (2008) [arXiv:0712.1475 [hep-ph]]; A.E. Bondar and V.L. Chernyak, Phys. Lett. B **612**, 215 (2005); V.V. Braguta, A.K. Likhoded and A.V. Luchinsky, Phys. Rev. D **74**, 094004 (2006); Phys. Rev. D **72**,

- 074019 (2005); D. Ebert and A.P. Martynenko, Phys. Rev. D **74**, 054008 (2006); H.-M. Choi and C.-R. Ji, Phys. Rev. D **76**, 094010 (2007).
- [43] Y. J. Zhang, Q. Zhao and C. F. Qiao, Phys. Rev. D **78**, 054014 (2008) [arXiv:0806.3140 [hep-ph]], X. H. Guo, H. W. Ke, X. Q. Li and X. H. Wu, arXiv:0804.0949 [hep-ph]. H. M. Choi and C. R. Ji, Phys. Rev. D **76**, 094010 (2007) [arXiv:0707.1173 [hep-ph]]. Y. Jia, Phys. Rev. D **76**, 074007 (2007) [arXiv:0706.3685 [hep-ph]].
- [44] G. T. Bodwin, D. Kang and J. Lee, Phys. Rev. D **74**, 114028 (2006) [arXiv:hep-ph/0603185].
- [45] F. Yuan, C. F. Qiao and K. T. Chao, Phys. Rev. D **56**, 321 (1997) [arXiv:hep-ph/9703438].
- [46] E. Braaten and Y. Q. Chen, Phys. Rev. Lett. **76**, 730 (1996) [arXiv:hep-ph/9508373].
- [47] B. Aubert *et al.* [BABAR Collaboration], Phys. Rev. Lett. **87**, 162002 (2001) [arXiv:hep-ex/0106044].
- [48] K. Abe *et al.* [BELLE Collaboration], Phys. Rev. Lett. **88**, 052001 (2002) [arXiv:hep-ex/0110012].
- [49] P. Cho and A.K. Leibovich, Phys. Rev. D **54**, 6690 (1996); F. Yuan, C.F. Qiao, and K.T. Chao, Phys. Rev. D **56**, 1663 (1997); S. Baek, P. Ko, J. Lee, and H.S. Song, J. Korean Phys. Soc. **33**, 97 (1998); V.V. Kiselev *et al.*, Phys. Lett. B **332**, 411 (1994); S.J. Brodsky, A.S. Goldhaber and J. Lee, Phys. Rev. Lett. **91**, 112001 (2003).
- [50] S. Fleming, A. K. Leibovich and T. Mehen, Phys. Rev. D **68**, 094011 (2003) [arXiv:hep-ph/0306139].
- [51] Z. H. Lin and G. h. Zhu, Phys. Lett. B **597**, 382 (2004) [arXiv:hep-ph/0406121].
- [52] A. K. Leibovich and X. Liu, Phys. Rev. D **76**, 034005 (2007) [arXiv:0705.3230 [hep-ph]].
- [53] P. Pakhlov *et al.* [Belle Collaboration], Phys. Rev. D **79**, 071101 (2009) [arXiv:0901.2775 [hep-ex]].
- [54] M. Böhm, A. Denner, J. Küblbeck, Comput. Phys. Commun. **60** (1990) 165; T. Hahn, Comput. Phys. Commun. **140**, 418 (2001).
- [55] R. Mertig, M. Böhm, A. Denner, Comput. Phys. Commun. **64** (1991) 345.
- [56] T. Hahn and M. Perez-Victoria, Comput. Phys. Commun. **118**, 153 (1999).
- [57] P. Ko, J. Lee and H. S. Song, Phys. Rev. D **54**, 4312 (1996) [Erratum-ibid. D **60**, 119902 (1999)] [arXiv:hep-ph/9602223].
- J.H. Kühn, J. Kaolan and E.G.O. Safiani, Nucl. Phys. **B157**, 125 (1979);
- B. Guberina, J.H. Kühn, R.D. Peccei and R. Rückl, Nucl. Phys. **B174**, 317 (1980).

- [58] S. Dittmaier, Nucl. Phys. B **675**, 447 (2003).
- [59] B. W. Harris and J. F. Owens, Phys. Rev. D **65**, 094032 (2002) [arXiv:hep-ph/0102128].
- [60] P. L. Cho and A. K. Leibovich, Phys. Rev. D **53**, 150 (1996) [arXiv:hep-ph/9505329].
- [61] P. L. Cho and A. K. Leibovich, Phys. Rev. D **53**, 6203 (1996) [arXiv:hep-ph/9511315].
- [62] E. Braaten, B. A. Kniehl and J. Lee, Phys. Rev. D **62**, 094005 (2000) [arXiv:hep-ph/9911436].
- [63] M. Kramer, Prog. Part. Nucl. Phys. **47**, 141 (2001) [arXiv:hep-ph/0106120].